Pore Structure Development during Hydration of Tricalcium Silicate by X-ray Nano-imaging

Wei Lin[1], Bo Chen*[,1,2], Xianping Liu*[,1,3], Francesco Iacoviello[4], Paul Shearing[4] and Ian Robinson[1,2,5]

[1]School of Materials Science and Engineering, TongJi University, Shanghai, 201804, China

[2]London Centre for Nanotechnology, University College, London, WC1H 0AH, UK

[3]Key Laboratory of Advanced Civil Engineering Materials (Tongji University), Ministry of Education, Shanghai, 201804, China

[4]Department of Chemical Engineering, University College, London, WC1E 6BT, UK

[5]Department of Condensed Matter Physics and Materials Science, Brookhaven National Laboratory, Upton, NY, 11973, USA

*Corresponding author: bo.chen@tongji.edu.cn (Bo Chen)
and lxp@tongji.edu.cn (Xianping Liu)

Key words

Hydration; Tricalcium silicate; Transmission X-ray Microscopy; Pore structure; porosity; cement

Abstract

Tricalcium silicate (C_3S) is the most important cement mineral phase among the four main clinker phases and the majority of cement formulations use it. Pure C_3S is widely used as a simplified model system of cement in various research studies. However, the structure development of cement during hydration at the nano-scale has been rarely reported. In this work, Transmission X-ray Microscopy (TXM), a nondestructive X-ray analysis method, was used to study the hydration of pure C_3S sample with a water/C_3S mass ratio of 0.5. The three-dimensional (3D) structure of hydrated C_3S sample was investigated, especially the internal pore structure development. 3D images have been obtained for the same sample of C_3S, 5 days and 28 days after hydration, which allows us to reveal the structure development of the hydrating C_3S, in three dimensions, includes the changes in pore sizes, shapes and the evolution of geometric structure of pores at different hydration times.

1. Introduction

The chemical reactions of Portland cement with water determines the setting and hardening behavior of the cement mortar and cement concrete, as well as the overall structure of these materials [1-4]. The internal spatial structure or morphologic organization produced by these reactions has been widely investigated in order to understand their impact on the setting and hardening process, and later on the materials properties and performance of the cement-based materials. Research has shown that the morphologic organization of cement-based materials has great impact on their mechanical and engineering properties and performance, sometimes even more important than their chemical composition [5-9]. In the cement-based materials,

the pore structure is a critical component, which determines the internal morphologic organization. Hence the pore structure directly affects the properties and performance of cement-based materials such as their impermeability, shrinkage, elastic modulus and strength [10,11]. Tricalcium silicate (C_3S), as the most important constituent of Portland cement, has been extensively investigated [12-16] because its hydration controls the setting and strength development of the cement-based materials. In our study, C_3S was used as a simplified model system of cement to investigate the internal pore structure development of the sample during the hydration process.

Direct observation of the changes in microstructure of cement-based materials is challenging for many experimental techniques. So far, microstructure of cement paste has been widely studied in order to have a better understanding of the cement hydration process and thus to develop better and more-dedicated cement based materials [17-22]. However, there are few reports on the internal pore structure of cement paste, especially at the nano-scale [23-25]. This is partly because it is extremely complex and disorderly and partly because it needs three-dimensional (3D) imaging. Although it is hard to precisely measure the porosity of cement paste, three methods were used to estimate this quantity: gas adsorption [26], mercury intrusion porosimetry (MIP) [27] and direct observation techniques including optical microscopy and scanning electron microscopy (SEM) [28-30]. Gas absorption and MIP only provide indirect measurements of pore structure. SEM, which is frequently used to characterize the cement materials, can only show the pores in two-dimensional images. Despite these observations being of great insight, it has not been possible to make direct observations of the evolution of the structure over time. In addition, these imaging techniques require careful sample preparation that may also introduce artifacts.

After all these works completed so far, agreement is still not reached even about the basic mechanisms of cement hydration due to a lack of sufficiently detailed experimental observations, especially of the temporal evolution of the microstructure of cement-based materials [31-34]. This paper presents the use of Transmission X-ray Microscopy (TXM) to direct observe the morphological evolution of a cement paste model as a function of hydration time in order to enrich our knowledge of the underlying hydration mechanism at the materials level.

2. Experimental procedures

Transmission X-ray microscopes (TXM), a sophisticated technique, uses an instrumental setup which is shown in **Fig.1**. In our investigation, TXM records the X-ray absorption projections of target objects in the forward transmission geometry, using a Fresnel Zone Plate (FZP) as a projection lens with high magnification, as a function of rotation angle. It then reconstructs a 3D image using the computed tomography (CT) back-projection algorithm. Although more advanced X-ray imaging modes exist [35-37], common to all of them is that the resolution is limited by the quality of X-ray optics currently available. For example, generally increasing the size of the X-ray optics usually has a positive effect on the spatial resolution [38]. Zernike phase contrast (ZPC) is a microscopy technique that produces phase contrast by converting phase modulations in the image into detectable amplitude modulations

[39]. In modern TXM set-ups, ZPC is introduced using a phase ring [40,41]. In the work reported here, TXM was used to observe microstructure of a model cement-based materials in 3D.

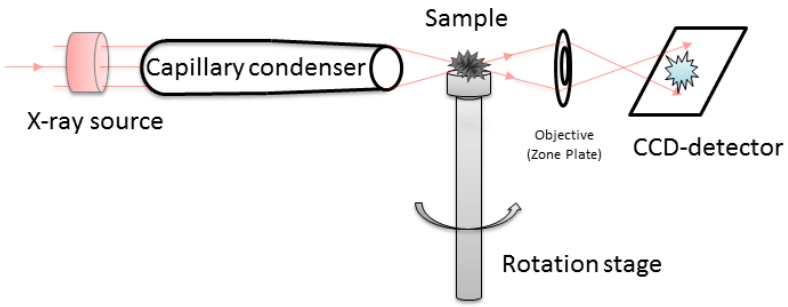

Fig. 1 A schematic diagram of the transmission X-ray microscopy setup.

Pure monoclinic C_3S powder was synthesized at the School of Materials Science and Engineering, Tongji University, following the experimental procedure reported by De la Torre & Aranda [42]. The specimen was stored in a small sealed box at room temperature with desiccant before the X-ray experiment. The microscale cement paste specimen was specially prepared with a water to cement ratio of 0.5 in a capillary tube of 100μm diameter. The pore microscale structure was characterized by using an Xradia Ultra X-ray microscope in University College London (UCL).

The preparation of Nano-scale TXM specimens is a challenging task requiring special procedures. A special procedure was carried out to meet the specimen size constraint by injecting the fresh cement paste into a glass thin-walled capillary tube with an inner diameter of 0.08 mm and a wall thickness of 0.01 mm, designed for the X-ray diffraction with a photon energy of 10 keV. It should be pointed out that the injection tends to bring more water into the tube. After that, the specimen was sectioned immediately to a length of 1 mm to avoid capillary effects. This short section of cement paste was immersed into water for curing. The sample was examined twice with TXM, after 5 days and 28 days of curing. During the curing processes, the hardened cement paste specimens were kept in the sealed box with desiccant before performing the TXM image acquisition.

The sample was mounted on a stage with four degrees of freedom: x, y, and z translations for positioning and centering of the sample, and rotation for data acquisition. The rotary stage allows for many X-ray transmission images of the sample to be recorded at a sequence of orientations. The absorption contrast imaging setting was used for the measurements. This generates contrast in the images based on the differential attenuation properties of the matter in the sample.

3. Results and discussion

3.1 A general analysis of the structure of the cement paste

With X-ray energies sufficient to penetrate through the entire cement specimen, a series of 2D projection images taken from sample in different orientations about a fixed rotation axis,

which can be used for 3D sample reconstructions in the form of a tomogram. **Fig.** 2 shows the projection images and reconstructed and cross-sectional images of the cement specimen at both hydration times in **Fig.** 2 a-f. **Fig.** 2c and f are segmented from **Fig.** 2b and d using the software package ‘‘Avizo’’[43]. The dark part seen in **Fig.** 2 is the air which surrounding the specimen, as well as the pore space inside the specimen. Among those dark parts, the pore space inside the specimen is colored in **Figs.** 2c and f as red, purple, green, dark blue and light blue. The lighter parts in **Fig.** 2a, b, d and e, has higher density, represents the solid phase of the cement specimen, i.e. the cement hydrates and unhydrated cement particles which are shown as yellow in **Fig.** 2c and f.

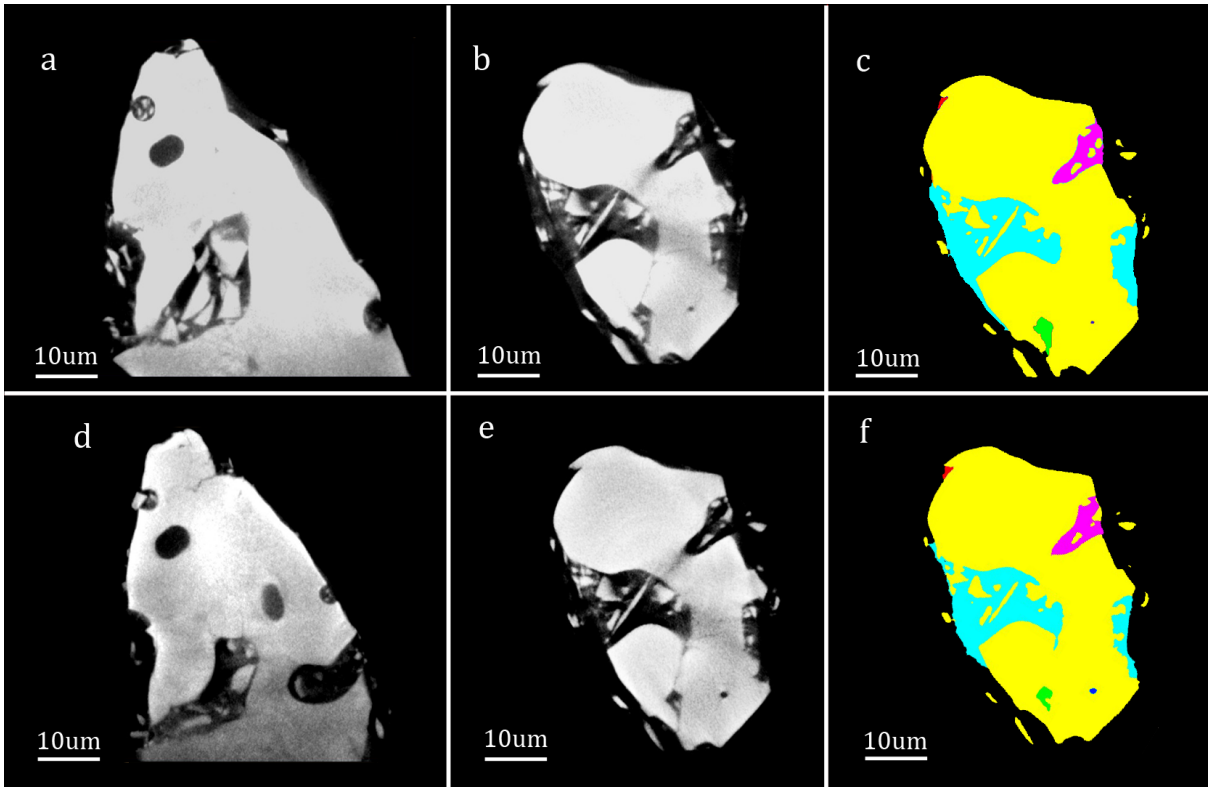

Fig. 2 Tomogram images and reconstructed cross-sectional images. **(a, b)** 5 days post hydration; **(c)** segmented result from Fig. 2b; **(d, e)** 28 days post hydration, **(f)** segmented result from Fig. 2e.

Fig. 3 presents the rendered images of the reconstructed volume of the specimen. For both hydration times, we can clearly see the whole morphology of the cement paste from the outside in **Fig.** 3a and d. The 3D spatial structure of the pores inside the specimen are shown in **Fig.** 3b, c, e and f. After calculation which runs in software Avizo, the “volume3d” results which represents the volume of a segmented object are given in **Table 1**. Generally from the outside, the shape of the whole cement specimen looks similar at both times. From Table 1, it can be seen that the total volume of the sample (solid and pores) increased from 45162 um^3 after 5 days hydration to 45214 um^3 after 28 days hydration. The fraction of pores

was seen to decrease as hydration time went from 5 days to 28 days with a clear change in the shapes and sizes of the pores.

Previous research has suggested that the hydration process occurs not only on the surface, but also on the inside of cement paste formulations, although the techniques used cannot resolve the specific location and is only roughly quantitative [44,45]. Our result shows a clear variation of shape and spatial distribution of each pore, which will be discussed with detail in the next sections.

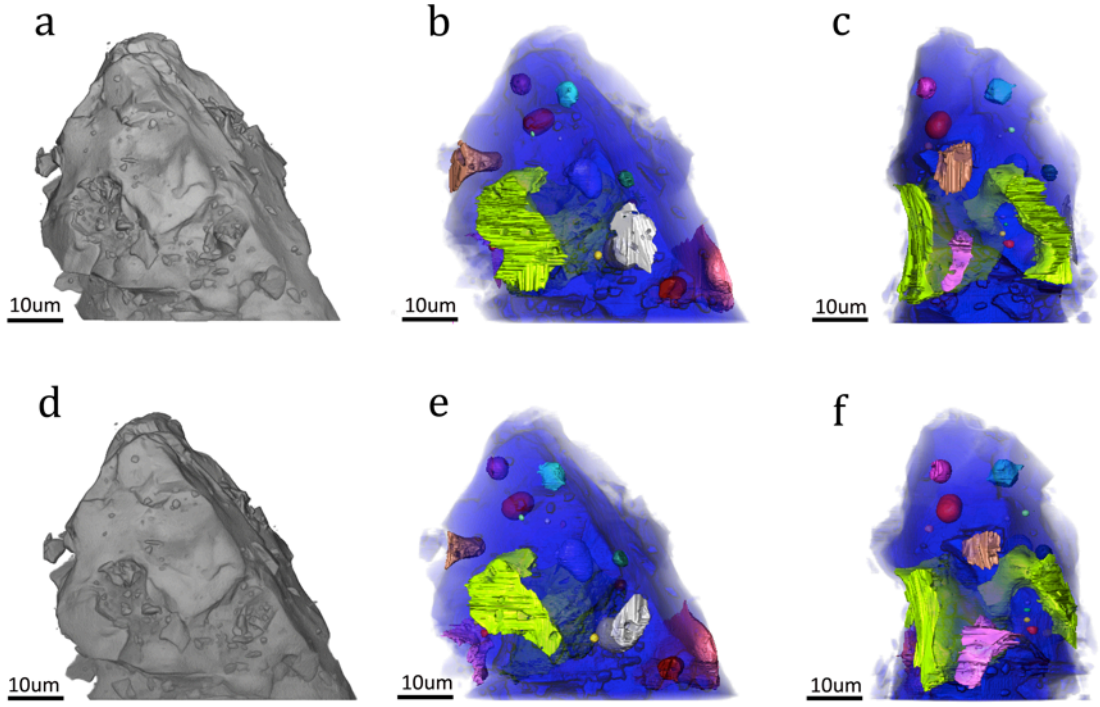

Fig. 3 Rendering of 3D volume images of cement specimen. 5 days hydration in **(a)**original form, **(b, c)** after segmentation; 28 days hydration days in **(d)** original form, **(e, f)** after segmentation

Table 1 the volume results of the cement paste in both hydration time

	Porosity (%)	Solid phase (um^3)	Pores (um^3)
5 days	9.82	40725	4437
28 days	9.13	41083	4130

3.2 Shape and spatial distribution of pores

Fig. 4 presents 3D renderings after segmentation, analogous to **Fig.** 3, showing the distribution of pores in more detail. We identified 21 pores in total, which are labeled A to U in **Fig.** 4. We can see pores with different size and shape scattered within the sample which cannot be classified in 2D slice images. We define two types of pores: sealed pores, surrounded by cement, and open pores, which have at least one path exposed to the atmosphere. Pores E, F, I, L, M, N, O, R, S, T and U are sealed, while the others are open pores. Not surprisingly, the open pores are distributed in the outer layer of the sample. Pore A, by far the largest pore, penetrating the whole sample becomes longer and narrower as

hydration time went on from 5 days to 28 days. The sealed pores are found to be distributed randomly within the model cement specimen and are not found to change very much in time.

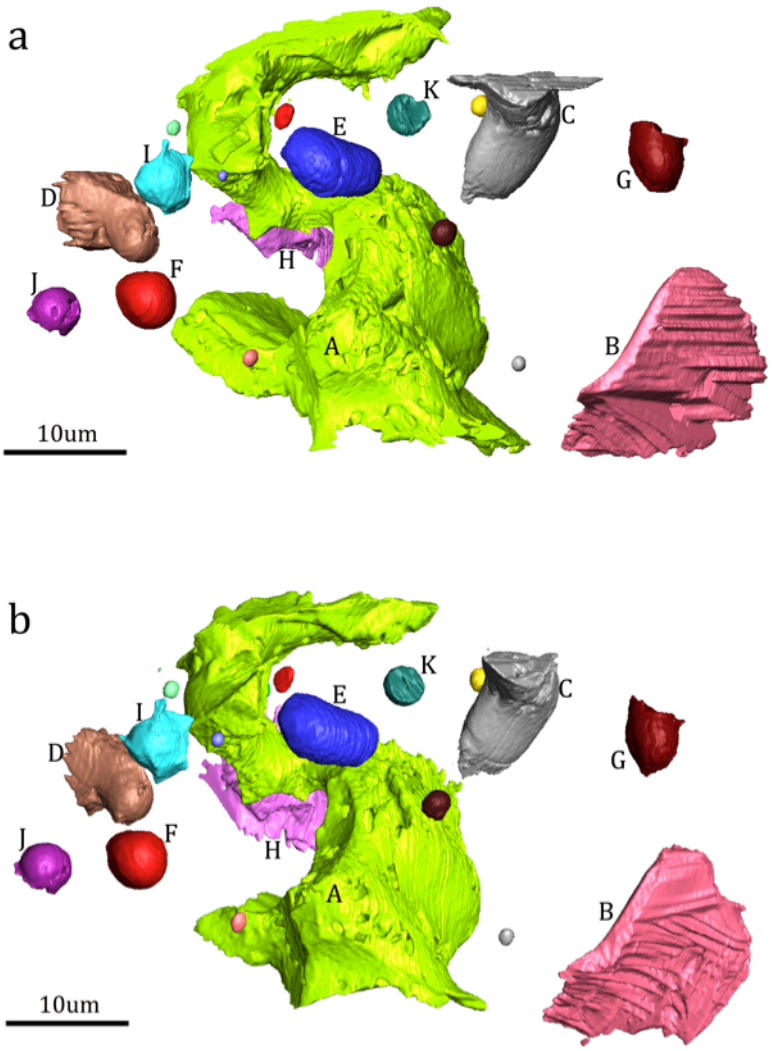

Fig. 4 Rendering of 3D spatial structure image of the pores inside the cement specimen after hydration for **(a)** 5 days and **(b)** 28 day

While the spatial arrangement of pores is clearly shown in **Fig.** 4, we still cannot easily identify the evolution of the position of each pore during hydration. To see these changes, we recorded the center of mass of each pore, reported by Avizo, to show the distance of pores from Pore E in **Fig.5**. We found that the pore positions barely changed during hydration. The result is consistent with the similar appearance of the pores in **Fig. 4**.

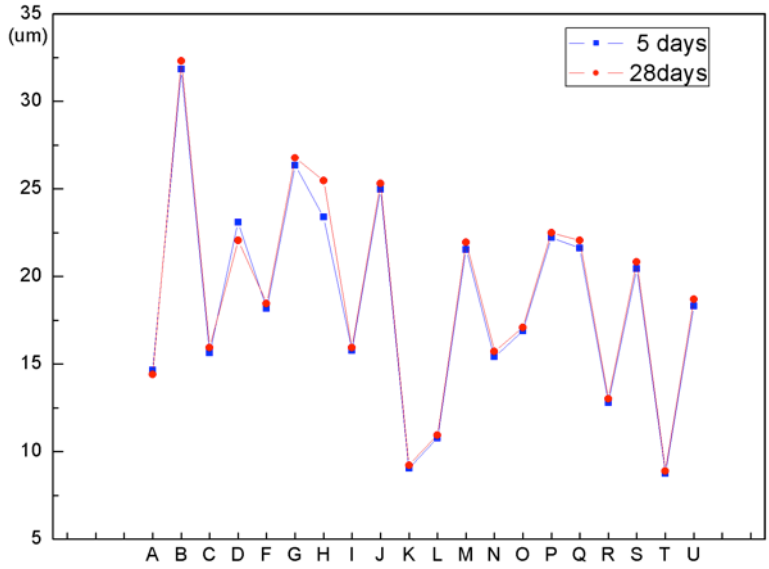

Fig. 5 Distance of pores from Pore E in the cement specimen examined after hydration for 5 days and 28 days

3.3 Structure quantification

The details of the 21 pores found in the specimen post hydration for both 5 days and 28 days are shown in table 2 in terms of the geometric parameters length(L), width(W), volume(V) based on the Feret method [43] and its percentage change between the two hydration states. Since these images were segmented manually, they may contain interpretation errors introduced inevitably. For a better accuracy of the subsequent analysis of the pore statistics, we take out the pores with the highest (pore H) and lowest (pore D) value of percentage change.

The sealed pores, E, F, I, L, M, N, O, P, Q, R, S, T and U, all grow bigger in time. The open pores mostly become smaller, except for J. Pore A, the largest pore, is seen to get longer and narrower. This results in the volume of pore A becoming massively reduced, and dominates the change in porosity in table 1. For Pore B, the length and width are both increased. However, the length and width in Table2 are the longest and shortest Feret diameter of pores respectively, the volume turns out to be decreased; Pore C is decreased in length and volume, while getting larger in width; Pore G and K are both decreased in width and volume, but increased in length.

The samples were prepared with sufficient water to allow the hydration reaction to continue during the whole experiment. For the water-accessible open pores, it seems reasonable that the hydration products will continue to grow and fill the solid phase of cement over time. So, the increasing volume of the solid phase and the decreasing size of the open pores are expected results. On the other hand, autogenous chemical shrinkage could be responsible for the growing size of sealed pores over time. Because a cement paste hydrating under sealed conditions will self-desiccate, this creates empty pores within the hydrating paste due to loss of water [46]. And the amount of the absorbed water corresponds to the chemical shrinkage, since the hydration products formed during the hydration of cement occupy less space than the corresponding reactants [47]. This phenomenon, chemical

shrinkage, also leads to tensile stresses through the formation of menisci, which is critical to the shrinkage of cement. Although pore J is open to atmosphere, but most of the surface is in contact with the cement and available to form menisci. This can also explain why the size of pore J get increased not like other open pores.

Table 2 Pore size of C3S after hydration for 5days and 28days

		5 Days				28 Days			Change
		L(μm)	W(μm)	V(μm^3)		L(μm)	W(μm)	V(μm^3)	(%)
1	A	43.1	26.0	2980.8	A	45.5	24.5	2625.6	-14
2	B	22.1	10.8	615.1	B	22.8	11.7	605.2	-02
3	C	17.2	8.9	278.7	C	15.9	7.5	244.5	-14
4	D	12.0	7.8	158.8	D	10.1	6.8	93.7	-70
5	E	8.4	5.0	122.8	E	9.0	5.5	136.9	+10
6	F	6.4	4.5	73.1	F	6.5	4.8	80.6	+09
7	G	6.7	5.1	55.3	G	8.6	4.9	49.1	-12
8	H	13.3	6.6	52.3	H	18.4	8.5	166.0	+69
9	I	6.9	4.3	47.8	I	10.8	5.3	63.7	+25
10	J	5.0	3.8	24.3	J	7.4	4.4	32.7	+26
11	K	3.8	2.8	12.4	K	4.0	2.7	12.3	- 01
12	L	2.5	2.1	5.2	L	2.9	2.3	6.8	+24
13	M	2.5	1.6	2.8	M	2.8	1.7	3.1	+10
14	N	2.0	1.7	2.6	N	2.4	1.9	3.2	+17
15	O	1.7	1.2	1.2	O	2.0	1.2	1.6	+21
16	P	1.5	1.2	1.0	P	1.8	1.3	1.3	+24
17	Q	1.4	1.1	0.7	Q	1.5	1.1	0.7	+01
18	R	1.4	1.0	0.7	R	3.7	1.4	1.2	+41
19	S	1.6	1.0	0.6	S	1.3	1.1	0.6	+00
20	T	1.1	0.9	0.4	T	1.4	1.2	0.9	+57
21	U	1.1	0.8	0.3	U	1.7	0.9	0.5	+43

4. Conclusion

Transmission X-ray microscopy (TXM) is shown to be a useful tool for the nondestructive investigation of the porosity and morphology of cement materials over the long time periods needed to study the slow structural changes associated with cement hardening. It is demonstrated to provide detailed morphological information on pore shape, porosity, size and spatial distribution of pores within a cement-based model material. These features changed by small fractions but significantly as hydration time went on from 5 days to 28 days. TXM provides three dimensional images, as required to understand the development of the pore microstructure. In our work, evidence has been presented that hydration process occurs not only on the surface, but also inside the bulk of the C_3S cement paste with solid quantification. The position of each pore shows no significant change during the process of hydration in our

experiment. Importantly, two types of pores were defined in our research: open pores and sealed pores depending on whether they were connected with the outside atmosphere. Significantly, we found a general trend that the size of sealed pores grows bigger, while the open pores become smaller between the two hydration times.

Acknowledgment

We thank Andrew Chiu for helping with the measurements. This work was supported by the TongJi University's Talent Program "Materials Nanostructure" with grants 152221 and 152243, and the UK Engineering and Physical Sciences Research Council (EPSRC) grant EP/I022562/1 "Phase modulation technology for X-ray imaging". Work performed at Brookhaven National Laboratory was supported by the US Department of Energy, Office of Basic Energy Sciences, under Contract Number DE-SC00112704. Part of the work at TongJi University was also supported by the National Natural Science Foundation of China grant 51102181. XL was supported by the State Scholarship Fund of China when implementing the experiment.

References

[1] Barnes P, Bensted J (2002) Structure and performance of cements, Edition 2, Chapter3, CRC Press: 57-113
[2] Taylor H F W (1997) Cement chemistry, Edition 2, Thomas Telford
[3] Gartner E M, Gaidis J M (1989) Hydration Mechanisms, I; in Materials Science of Concrete, Edited by J. Skalny. American Ceramic Society, Westerville, OH, 1: 95–125
[4] Bullard J W, Jennings H M, Livingston R A, Nonat A, Scherer G W, Schweitzer J S, Scrivener K L, Thomas J J (2011) Mechanisms of cement hydration, Cem Concr Res 41:1208–1223
[5] Maruyama I, Nishioka Y, Igarashi G, Matsui K (2014) Microstructural and bulk property changes in hardened cement paste during the first drying process. Cem Concr Res 58: 20-34
[6] Sumanasooriya M S, Neithalath N (2009) Stereology- and morphology-based pore structure descriptors of enhanced porosity (pervious) concretes. ACI Mater J 106(5)
[7] Hu J (2004) Porosity of concrete, morphological study of model concrete. PhD thesis, Delft University, the Netherlands
[8] Neithalath N, Marolf A, Weiss J, Olek J (2005) Modeling the influence of pore structure on the acoustic absorption of enhanced porosity concrete. J Adv Concr Technol 3:29-40
[9] Lu S, Landis E N, Keane D T (2006) X-ray microtomographic studies of pore structure and permeability in Portland cement concrete. Mater Struct 39:611–620
[10] Hansen T C (1986) Physical structure of hardened cement paste. A classical approach. Mater Struct 19(6); 423-436
[11] Xi Y, Siemer D D, Scheetz B E (1997) Strength development hydration reaction and pore structure of autoclaved slag cement with added silica fume. Cem Concr Res 27(27): 75-82

[12] Slegers P A, Genet M, Léonard A J, Fripiat J J (1977) Structural transformation of tricalcium silicate during hydration. Appl Cryst 10:270-276
[13] Taylor H F W, Barret P, Brown P W et al (1984) The hydration of tricalcium silicate. Mater Struct 17: 457–468
[14] Dent Glasser L S, Lachowski E E, Mohan K, Taylor H F W (1978) A multi-method study of C3S hydration. Cem Concr Res 8(6): 733-739
[15] Livingston R A, Schweitzer J S, Rolfs C, Becker H W, Kubsky S (2001) Characterization of the induction period in tricalcium silicate hydration by nuclear resonance reaction analysis. Mater Res 16(3): 687–93
[16] Damidot D, Bellmann F, Mo¨ser B, Sovoidnich T (2007) Calculation of the dissolution rate of tricalcium silicate in several electrolyte compositions. Cem Wapno Beton 12/74 (2): 57–67
[17] Holzer L, Gasser P H, Kaech A, Wegmann M, Zingg A, Wepf R, Muench B (2007) Cryo-FIB-nanotomography for quantitative analysis of particle structures in cement suspensions. J Micrsc-Oxford 227: 216–228;
[18] da Silva J C, Trtik P, Diaz A et al (2015) Mass Density and Water Content of Saturated Never-Dried Calcium Silicate Hydrates. Langmuir, 31: 3779−3783
[19] Cuesta A, De la Torre A G, Santacruz I et al (2017) Chemistry and mass density of aluminum hydroxide gel in Eco-Cements by Ptychographic X□ray computed tomography. Phys Chem C 121: 3044−3054
[20] Bentz D P (1997) Three□dimensional computer simulation of Portland cement hydration and microstructure development. J Am Ceram Soc 1: 3-21
[21] Suna W, Houa K, Yanga Z, Wenb Y (2017) X-ray CT three-dimensional reconstruction and discrete element analysis of the cement paste backfill pore structure under uniaxial compression. Constr Build Mater 138: 69–78
[22] Hu Q, Aboustait M, Kim T, Tyler Ley M, Hanan J C, Bullard J, Winarski R, Rose V (2016) Direct three-dimensional observation of the microstructure and chemistry of C3S hydration. Cem Concr Res 88:157–169
[23] Pavel T, Ana D, Manuel G, Andreas M, Oliver B (2013) Density mapping of hardened cement paste using ptychographic X-ray computed tomography, Cement & Concrete Composites 36 :71–77
[24] Nathan B, Perrine C, Jérôme V, Daniel B, Clément L et al (2015) Micro- and nano-X-ray computed-tomography: A step forward in the characterization of the pore network of a leached cement paste, Cement and Concrete Research 67: 138–147
[25] Yan-Shuai W, Jian-Guo D (2017) X-ray computed tomography for pore-related characterization and simulation of cement mortar matrix, NDT&E International 86: 28–35
[26] Juenger M, Jennings H (2001) The use of nitrogen adsorption to assess the microstructure of cement paste. Cem Concr Res 31: 883–92
[27] Abell A B, Willis K L, Lange D A (1999) Mercury intrusion porosimetry and image analysis of cement-based materials. J Colloid Interface Sci 211:39-44
[28] Bailey J E, Stewart H R (1984) C_3S hydration products viewed using a cryo stage in SEM. J Mater Sci Lett 3(5): 411–414

[29] Lawrence F V, Young J F (1973) Studies on the hydration of tricalcium silicate pastes: I. Scanning electron microscopic examination of microstructural features. Cem Concr Res 3(2):149 ± 161.
[30] Jennings H M, Dalgleish B J, Pratt P L (1981) Morphological development of hydrating tricalcium silicate as examined by electron microscopy. J Am Ceram Soc 64 (10): 567 ± 572
[31] Bullard J W, Scherer G W, Thomas J J (2015) Time dependent driving forces and the kinetics of tricalcium silicate hydration. Cem Concr Res 74: 26–34
[32] Scherer G W, Zhang J, Thomas J J (2012) Nucleation and growth models for hydration of cement. Cem Concr Res 42: 982–993
[33] Thomas J J, Biernacki J J, Bullard J W, Bishnoi S, Dolado J S, Scherer G W, Luttge A (2011) Modeling and simulation of cement hydration kinetics and microstructure development. Cem Concr Res 41: 1257–1278
[34] Bullard J W (2008) A determination of hydration mechanisms for tricalcium silicate using a kinetic cellular automation model. J Am Ceram Soc 91: 2088–2097
[35] Robinson I, Harder R (2009) Coherent X-ray diffraction imaging of strain at the nanoscale. Nature Mater 8: 291-298
[36] Shapiro D A, Yu Y S, Tyliszczak T (2014) Chemical composition mapping with nanometre resolution by soft X-ray microscopy. Nature Photon 8: 765–769
[37] Thibault P, Dierolf M, Menzel A, Bunk O, David C, Pfeiffer F (2008) High-resolution scanning X-ray diffraction microscopy. Science, 321(5887): 379-382
[38] Hopkins H H, Barham P M (1950) The influence of the condenser on microscopic resolution. P Phys Soc Lond B 63(370):737–744
[39] Zernike F (1942) Phase contrast, a new method for the microscopic observation of transparent objects. Physica 9(7): 686–698
[40] Neuhäusler U, Schneider G, Ludwig W, Meyer M A, Zschech E, Hambach D (2003) X-ray microscopy in Zernike phase contrast mode at 4keV photon energy with 60nm resolution. J Phys D: Appl Phys 36: 79-82
[41] Vartiainen I, Mokso R, Stampanoni M, David C (2014) Halo suppression in full-field x-ray Zernike phase contrast microscopy. Opt Lett 39(6): 1601-1604
[42] De la Torre A G, Aranda M A G (2003) Accuracy in Rietveld quantitative phase analysis of Portland cements. J Appl Cryst 36: 1169-1176
[43]https://www.fei.com/software/avizo-for-materials-science/
[44] Juenger M C G, Monteiro P J M, Gartner E M, Denbeaux G P (2005) A soft X-ray microscope investigation into the effects of calcium chloride on tricalcium silicate hydration. Cem Concr Res 35: 19–25
[45] Silva D A, Monteiro P J M (2006) The influence of polymers on the hydration of Portland cement phases analyzed by soft X-ray transmission microscopy. Cem Concr Res 36: 1501–1507
[46] Bentz D P, Jensen O M (2004) Mitigation strategies for autogenous shrinkage cracking. Cem Concr Compos 26(6): 677-685
[47] Tazawa E, Miyazawa S, Kasai T (1995) Chemical shrinkage and autogenous shrinkage of hydrating cement paste. Cem Concr Compos 25(2) 288-292